Origin of Excess Light Scattering in Poly(methyl methacrylate) Glasses

Yasuhiro Koike,*,† Shiro Matsuoka,‡ and Harvey E. Bair‡

Faculty of Science and Technology, Keio University, Kohokuku, Yokohama 223, Japan, and AT&T Bell Laboratories, Murray Hill, New Jersey 07974

Received March 9, 1992

ABSTRACT: The origin of the excess light scattering invariably observed in purified poly(methyl methacrylate) (PMMA) glasses was investigated. The isotropic heterogeneous structure with a dimension of about 1000 Å, which increases the scattering loss by at least 1 order of magnitude (to several hundred dB/km), is generated during polymerization below T_g at high conversion and is not due to high molecular weight, specific tacticities, formation of cross-links, or aging. It is clearly shown that the remaining monomer in concentrations of several weight percent does not aggregate spontaneously at high conversion to cause excess scattering unless polymerization takes place. The excess scattering is, we believe, mainly due to voids caused by the volume shrinkage accompanying polymerization of the remaining monomer trapped inside the polymer glass. The excess scattering model proposed in this paper shows that if a slight amount of monomer in the PMMA glass is polymerized in situ at high conversion, generating slightly localized voids due to the aggregation of the unreacted initiator, a rise of only 1 wt % in the conversion increases the scattering loss by several hundred dB/km, which can reasonably explain the experimental results obtained in this paper.

Introduction

Light scattering of amorphous optical polymer glasses such as poly(methyl methacrylate) (PMMA), polystyrene (PSt), polycarbonate (PC), etc., has been widely studied[1-8] to investigate the local structures in the range between hundreds to thousands of angstroms. Especially, PMMA has received much attention because of its use for low-loss optical polymer waveguides[9-11] and as a core material of polymer optical fibers.[12-14] However, even in the highly purified PMMA glasses in which no anisotropic domains such as bundles of parallel molecular chains or folded chains have been observed by neutron or X-ray scatterings,[1,15] large-size heterogeneities with the dimension of about 1000 Å have been invariably observed by the angular dependence of polarized light scattering (V_V).[5,16,17] These large-size heterogeneities increase the light scattering loss up to several hundred dB/km in the range of visible light, although the isotropic scattering loss estimated from the thermal density fluctuation theory by Einstein,[18] eq 1, is only 9.5 dB/km at 633-nm wavelength.

$$V_V^{iso} = \frac{\pi^2}{9\lambda_0^4}(n^2-1)^2(n^2+2)^2 kT\beta \qquad (1)$$

where V_V^{iso} is the isotropic part of V_V, n the refractive index of the polymer, k Boltzmann's constant, T the absolute temperature, β the isothermal compressibility, and λ_0 the wavelength of light in vacuum.

In order to explain the excess light scattering of the PMMA caused by these large-size heterogeneities, many speculations have been proposed so far, e.g., the stereoregularity according to the configuration of specific tacticities, the effect of high molecular weight, low molecular weight impurities such as residual monomer or additives, the formation of cross-links or bulky side chains as the result of the "gel effect" during polymerization, internal frozen strain, etc. We reported[8] that, with an increase in the polymerization temperature from 60 to 130 °C, the V_V scattering remarkably decreased, while the weight-average molecular weight M_w, the polydispersity M_w/M_n, and the remaining monomer decreased, and the tacticity approached the random configuration. Therefore, several effects proposed as the origin of the excess scattering varied simultaneously, which made the independent analysis difficult. In spite of extensive work directed to understand this excess scattering, the origin of the large heterogeneous structure is still obscure.

In our previous paper,[8] PMMA glass in which no large-size heterogeneities (i.e., no angular dependence of V_V) existed was prepared for the first time. The isotropic scattering loss of this sample was ca. 10 dB/km, much smaller than any previously reported data and very close to the loss 9.5 dB/km from eq 1, which proved the validity of the thermal density fluctuation theory even in polymer glasses below T_g.[19] Thus, it became possible to investigate each hypothesized explanation of the origin of the excess scattering. The following were confirmed:

(a) Scattering losses (up to 400 dB/km) of samples having different tacticities and different molecular weights were reduced to almost the same value which was close to 9.5 dB/km by a sufficient heat treatment above T_g. Since the tacticity and molecular weight are not changed by the heat treatment, the excess scattering is intrinsically independent of these effects in the ranges of $M_w = 4 \times 10^4$–1.2×10^5 and P_h/P_s (the heterotactic to syndiotactic ratio) = 0.69–0.93.

(b) Small molecules such as the remaining monomer present in concentrations of a few weight percent do not seriously affect the excess scattering when they are not localized.

(c) The formation of cross-links as the result of the gel effect was not observed even in the sample with a large excess scattering.

On the basis of our previous study, the purpose of this paper is to quantitatively investigate the origin of such excess scattering in PMMA glasses, by proposing a model for the formation of the heterogeneous structure at high conversion when the polymerization is carried out below T_g. The ambiguous origin of the excess scattering invariably observed in the PMMA glasses may become, we believe, clear in this paper.

* To whom all correspondence should be addressed.
† Keio University.
‡ AT&T Bell Laboratories.

0024-9297/92/2225-4807$03.00/0

Experimental Section

Materials. In order to eliminate the effect of unknown impurities on the light scattering, a rigorous purification was carried out as follows: Inhibitors in the MMA monomer were removed by washing with 0.5 N NaOH aqueous solution, followed by washing out the residual NaOH with pure water until a neutral pH was achieved. The monomer was dried over Na_2SO_4, filtered through a 0.2-μm-membrane filter, and distilled [bp 46–47 °C (100 mmHg)] into a clean ampule A. Ampule A containing the purified monomer was connected to two clean ampules B and C. Di-*tert*-butyl peroxide (DBPO) as an initiator and *n*-butylmercaptan (nBM) as a chain-transfer agent were placed in ampule B, and ampule C was empty. Ampules A and B were frozen with liquid nitrogen, evacuated, and then purged with clean nitrogen. Then the contents in ampules A and B was degassed by several freeze–thaw cycles and slowly transferred as vapors into ampule C (a 20-mm inner diameter) under vacuum by cooling ampule C with liquid nitrogen. Finally, ampule C was sealed under vacuum and immersed in heated silicone oil for polymerization.

Light Scattering Measurement. The light scattering intensity was measured by an apparatus described in detail elsewhere.[8] The PMMA sample was placed in the center of the cylindrical glass cell, and the gap between the sample and the inner wall of the glass cell was filled with immersion oil with a refractive index of 1.5. This glass cell was perpendicularly located at the center of the goniometer, and a parallel beam of vertically polarized He–Ne laser (wavelength λ_0 = 633 nm) was injected from the side. In this paper, polarized (V_V) and depolarized (H_V) scattered light intensities were measured, in the range of scattering angle θ from 30 to 120°. To estimate the absolute intensity, pure benzene purified in the same manner as the monomer mixture was used as a standard for calibration.

Other Measurements. The molecular weight of the polymer was measured by gel permeation chromatography (GPC) (column; Showa Denko Co., Shodex AC-80M). The glass transition temperature (T_g) was measured by a differential scanning calorimeter (DSC, Perkin-Elmer DSC-2). The weight percent and identification of the remaining monomer in the PMMA glass was measured by a gas chromatograph/mass spectrometer (GC/MS) (Hewlett Packard 5995c) equipped with a cross-linked methyl silicone column (0.2-mm diameter, 12-m length) as follows: The polymer sample was dissolved in a small amount of acetone, followed by addition of methanol to precipitate the polymer. The monomer concentration in the supernatant was determined from the corresponding peak area of the chart of the gas chromatograph, and the structure of the monomer at this peak was identified by the mass spectrometer.

Analytical Procedure. In structureless liquids or randomly oriented polymers, the isotropic part V_{V1}^{iso} of the V_V scattering is given by[20]

$$V_{V1}^{iso} = V_{V1} - \frac{4}{3}H_V \tag{2}$$

Many PMMA samples prepared in this paper strongly exhibited the forward excess V_V scattering, while H_V scattering showed no angular dependence in its intensity. Therefore, it should be noted that the large-size heterogeneities causing the excess scattering are isotropic structures and are not due to anisotropic domains such as bundled or folded polymer chains. Then eq 2 was employed for the analysis of our PMMA samples. Here we separated the observed V_V scattering intensity into three terms as shown in Figure 1, namely

$$V_V = V_{V1}^{iso} + V_{V2}^{iso} + \frac{4}{3}H_V \tag{3}$$

where V_{V1}^{iso} denotes the isotropic background intensity which is independent of the scattering angle θ, and V_{V2}^{iso} is the isotropic scattering with the angular dependence due to large-size heterogeneities.

V_{V2}^{iso} is most important to investigate the structure giving the excess scattering discussed in this paper. The angular dependence of the V_{V2}^{iso} intensity is caused by an interference effect due to the large-size heterogeneities. When two close parallel beams with a wavelength λ are scattered at i and j points to the same direction, the phase difference of these beams is $\nu(\mathbf{r}\cdot\mathbf{s}-\mathbf{s}_0)$. Here $\nu = 2\pi/\lambda$, $\mathbf{s}_0$ and $\mathbf{s}$ are the unit vectors having the directions of the incident and scattered beams, respectively, and $(\mathbf{r})$ is the vector connecting the two points i and j. Then a single secondary wave results, represented in complex form by $\exp[-i\nu(\mathbf{r}\cdot\mathbf{s}-\mathbf{s}_0)]$; the scattering intensity I_s then becomes[21]

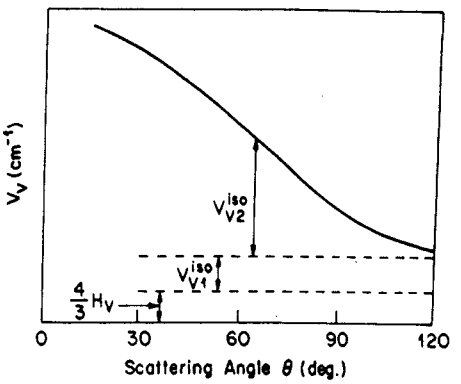

Figure 1. V_V scattering for polymer glass.

$$I_s = V\langle\eta^2\rangle\int_V \gamma(\mathbf{r})\exp[-i\nu(\mathbf{r}\cdot\mathbf{s}-\mathbf{s}_0)]\,d\mathbf{r} \tag{4}$$

where $\gamma(\mathbf{r})$ is the so-called correlation function introduced by Debye and Bueche and defined by eq 5.

$$\gamma(\mathbf{r}) = \frac{\langle\eta(\mathbf{r}_i)\cdot\eta(\mathbf{r}_j)\rangle_r}{\langle\eta^2\rangle} \tag{5}$$

Here $\eta(\mathbf{r}_i)$ and $\eta(\mathbf{r}_j)$ are the fluctuations of dielectric constants at the i and j positions which are a distance r apart, and $\langle\eta^2\rangle$ denotes the mean-square average of the fluctuation of all dielectric constants. Then eq 4 gives a general scattering intensity for any structure.

In the isotropic media with no long-range order which is our case, the average of $\exp[-i\nu(\mathbf{r}\cdot\mathbf{s}-\mathbf{s}_0)]$ in eq 4 becomes $\sin(\nu sr)/(\nu sr)$, $dV = 4\pi r^2\,dr$, and $V_{V2}^{iso} = (\pi^2 I_s)/(\lambda_0^4 V)$. Thus, $V_{V_2}^{iso}$ was given by Debye and Bueche[21] as

$$V_{V2}^{iso} = \frac{4\langle\eta^2\rangle\pi^3}{\lambda_0^4}\int_0^\infty \frac{\sin(\nu sr)}{\nu sr}r^2\gamma(r)\,dr \tag{6}$$

$$s = |\mathbf{s}-\mathbf{s}_0| = 2\sin(\theta/2)$$

$$\nu = 2\pi/\lambda$$

where λ and λ_0 are wavelengths of light in a specimen and under vacuum, respectively. In this paper, the correlation function $\gamma(r)$ is assumed to be approximated by eq 7 as suggested by Debye et al.[21] The validity of this assumption is discussed later.

$$\gamma(r) = \exp(-r/a) \tag{7}$$

where a is called the correlation length and is a measure of the size of the heterogeneities. Substituting eq 7 into eq 6 and integrating gives

$$V_{V2}^{iso} = \frac{8\pi^3\langle\eta^2\rangle a^3}{\lambda_0^4(1+\nu^2 s^2 a^2)^2} \tag{8}$$

The light scattering loss α is defined by

$$\alpha = -\frac{10}{y}\log\left(\frac{I}{I_0}\right) \tag{9}$$

where natural light with an intensity I_0 passes through a distance y and its intensity is decreased to I by only the light scattering. Differential of eq 9 gives

$$\alpha = (-10\log e)\left(\frac{1}{I}\frac{dI}{dy}\right) \tag{10}$$

Therefore, the scattering loss α corresponds to the decrease (dI) in light intensity (I) which is equal to the summation of light

scattered in all directions after passing through a distance dy. When the scattered light I_s from a unit scattering volume is detected on the differential surface dS at a distance R from the scattering point $dS = 2\pi(R \sin\theta)(R \cdot d\theta)$, then $(I_s/I)R^2 = (1/2)(V_V + V_H + H_V + H_H)$ and

$$\frac{1}{I}\frac{dI}{dy} = -\int \frac{I_s}{I} dS$$
$$= -\pi \int_0^{\pi} (V_V + V_H + H_V + H_H) \sin\theta \cdot d\theta \quad (11)$$

where the symbols V and H denote vertical and horizontal polarizations, respectively. Here the symbol A of the scattering component A_B is the direction of the polarizing phase of a scattered light and the subscript B is that of an incident light. θ is the scattering angle from the direction of the incident ray. In a randomly oriented polymer[22]

$$H_V = V_H \quad (12)$$

$$H_H = V_V \cos^2\theta + H_V \sin^2\theta \quad (13)$$

Then one obtains the scattering loss α expressed in terms of V_{V1}^{iso}, V_{V2}^{iso}, and H_V as follows:

$$\alpha = 10 \log e\pi \int_0^{\pi} \left\{ (1 + \cos^2\theta)(V_{V1}^{iso} + V_{V2}^{iso}) + \frac{(13 + \cos^2\theta)}{3} H_V \right\} \sin\theta \, d\theta \quad (14)$$

Now α is divided into three terms, α_1^{iso}, α_2^{iso}, and α^{aniso}.

$$\alpha = \alpha_1^{iso} + \alpha_2^{iso} + \alpha^{aniso} \quad (15)$$

where α_1^{iso} is the isotropic scattering loss from V_{V1}^{iso} with no angular dependence, α_2^{iso} is the isotropic scattering loss from V_{V2}^{iso} with angular dependence, and α^{aniso} is the anisotropic scattering loss from H_V. Since V_{V1}^{iso} and H_V have no angular dependence in their intensities, α_1^{iso} and α^{aniso} are simply calculated from eq 14 as follows:

$$\alpha_1^{iso} = 10 \log e\pi \int_0^{\pi} (1 + \cos^2\theta) V_{V1}^{iso} \sin\theta \, d\theta$$
$$= \frac{80}{3} \log e\pi V_{V1}^{iso} \quad (16)$$

$$\alpha^{aniso} = 10 \log e\pi \int_0^{\pi} \frac{(13 + \cos^2\theta)}{3} H_V \sin\theta \, d\theta$$
$$= \frac{800}{9} \log e\pi H_V \quad (17)$$

In the case of α_2^{iso}, substitution of eq 8 into eq 14 gives

$$\alpha_2^{iso} = 10 \log e\pi \int_0^{\pi} (1 + \cos^2\theta) V_{V2}^{iso} \sin\theta \, d\theta$$
$$= \frac{320 \log e a^3 \langle\eta^2\rangle \pi^4}{\lambda_0^4} \left\{ \frac{(b+2)^2}{b^2(b+1)} - \frac{2(b+2)}{b^3} \ln(b+1) \right\} \quad (18)$$

$$b = 4\nu^2 a^2$$

To determine the α_2^{iso} value, we first estimated the correlation length by the Debye plot of experimental data of V_{V2}^{iso} and $\langle\eta^2\rangle$ obtained by eq 8. Then these values were substituted in eq 18 to obtain α_2^{iso}.

Results and Discussion

Properties of Excess Scattering and Heterogeneities. To investigate the origin of the excess scattering in the PMMA glasses, we first have to clarify the properties of the excess scattering and heterogeneous structure generated below T_g. Figure 2 shows the change of the V_V and H_V intensities at the scattering angle $\theta = 60°$ (designated as V_{V60} and H_{V60}) as a function of polymerization time at high conversion, where the polymerization

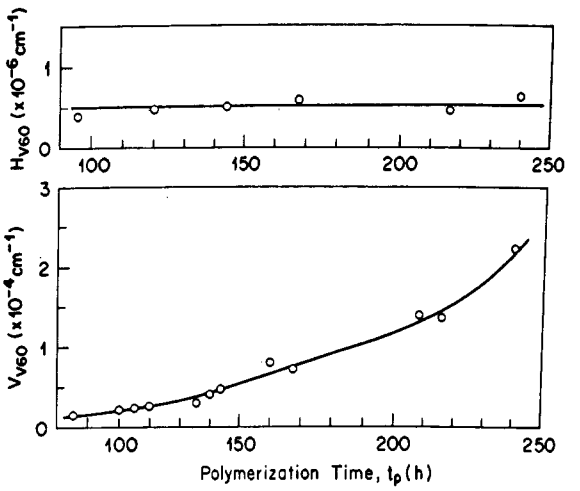

Figure 2. V_{V60} and H_{V60} scattering by PMMA glasses polymerized at 70 °C for t_p (h).

temperature (T_p) was 70 °C and the concentrations of DBPO and nBM were 0.2 wt %. (Unless otherwise noted, the concentrations of DBPO and nBM were both 0.2 wt % in this paper.) As pointed out by several researchers[16,23] in the polymerization at high conversion, the V_{V60} intensity in Figure 2 dramatically increased from 2×10^{-5} to 22×10^{-5} cm^{-1}, while the H_{V60} intensity remained the same at around 5×10^{-7} cm^{-1}. We think this large increase in the excess scattering of the sample polymerized below T_g at the final stage of polymerization should be a key element to solve the ambiguous problem about the excess scattering observed so far.

Insight into the nature of the last stages of the polymerization can be gained by examining the DSC behavior of PMMA polymerized at a temperature above and below PMMA's ultimate T_g of 108 °C (under the following sample conditions: monomer, <1 wt %; heating rate, 15 °C/min).

A comparative DSC scan of these two samples, one polymerized for 168 h at 70 °C (solid line, Figure 3) and the other reacted for 120 h at 130 °C (broken line, Figure 3), reveals the former (T_p = 70 °C) PMMA sample undergoes an exothermic reaction between 130 and 175 °C and liberates 14 J/g heat, whereas the latter (T_p = 130 °C) specimen does not. Note the sample that polymerizes has a T_g at about 84 °C and a small endotherm astride the glass transition interval due to physical annealing which occurs when T_p is lower than T_g.[24] These results indicate that the latter stages of the PMMA reaction carried out at 70 °C occurred in the glassy state. In contrast to this behavior the sample polymerized at 130 °C has a T_g just above 100 °C, and hence the latter stages of this reaction were not diffusion controlled.

From the heat of polymerization, ΔH_p, of 54 kJ/mol for PMMA and the residual heat measured for the sample polymerized at 70 °C we estimate 2.6 wt % of the MMA monomer reacted when heated above 130 °C.[25] GC/MS results (Table I) indicate heat treatment of this sample at 180 °C eliminated 3.3 wt % of the monomer. It is our contention that the structure which develops during the diffusion-controlled part of the reaction at 70 °C causes the observed excess scattering. At 70 °C, the half-life of DBPO is estimated to be greater than 17 000 h based on an activation energy of 31 kcal/mol. However, almost all the DBPO is utilized in 120 h at 130 °C. Hence, it is reasonable that nearly 3 wt % of the remaining 5 wt % of the MMA monomer reacts when heated above T_g.

Figure 4 shows the angular dependence of the V_V and H_V scattering of the samples polymerized at 70 °C where $s = 2 \sin(\theta/2)$. With an increase in the polymerization

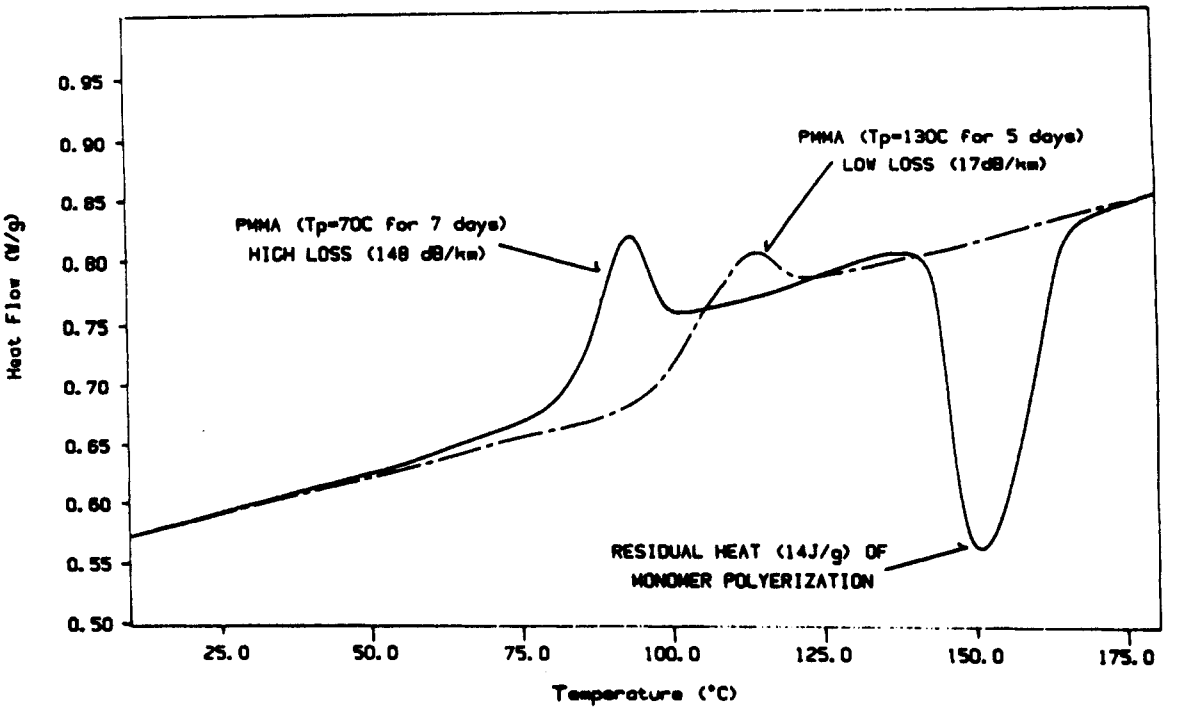

Figure 3. Comparative DSC scans of both low (T_p = 130 °C) and high (T_p = 70 °C) scattering loss PMMA samples.

Table I
Scattering Data and Physical Properties of PMMA Glasses Polymerized at 70 °C

t_p (h)	a (Å)	$\langle\eta^2\rangle$ (10^{-8})	V_{V1}^{iso} (10^{-5} cm^{-1})	H_v (10^{-7} cm^{-1})	α_1^{iso} (dB/km)	α_2^{iso} (dB/km)	α^{aniso} (dB/km)	α (dB/km)	T_g (°C)	monomer (wt %)
96	676	1.05	0.46	3.63	16.8	40.8	4.4	62.0	80	5.5
168	775	1.96	0.64	5.87	23.0	93.3	7.1	123	84	5.0
216	558	11.2	1.02	5.20	37.2	317	6.3	360	86	4.7
240	868	11.3	2.42	6.27	87.9	638	7.6	734	97	4.0
216[a]		0	0.24	3.31	8.9	0	4.0	12.9	102	1.7

[a] Heat treatment at 180 °C.

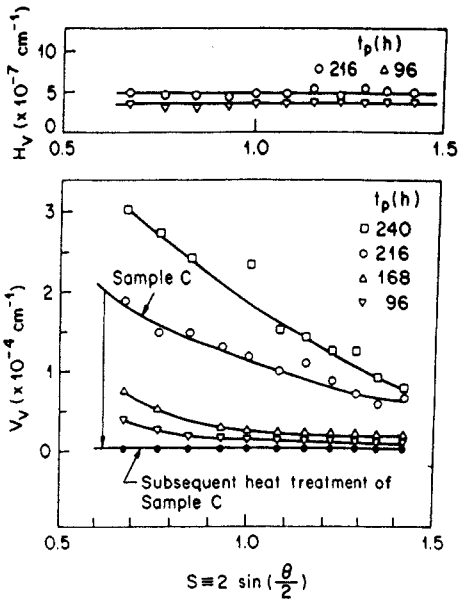

Figure 4. Angular dependence of V_V and H_V scattering by PMMA glasses polymerized at 70 °C for t_p (h).

time t_p, the V_V intensity showed an increasing angular dependence. However, when sample C polymerized at 70 °C for 216 h was heat-treated by increasing the temperature up to 180 °C, the V_V intensity remarkably reduced to 3 × 10^{-6} cm^{-1} and had no more angular dependence (● in Figure 4), which indicated the disappearance of the large-size heterogeneities during the heat treatment. Then we can say that the excess scattering is not due to extrinsic impurities, high molecular weight, formation of cross-links, or specific tacticities. On the other hand, the H_V scattering intensities for all samples had no angular dependence and were almost the same around 5 × 10^{-7} cm^{-1}. Therefore, it should be noted that the heterogeneous structures before the heat treatment were isotropic and no anisotropic order of polymer chains existed before or after the heat treatment.

As shown in Figure 1, it is assumed in our analytical procedure that V_{V2}^{iso} is superimposed on H_V and V_{V1}^{iso}. By the rearrangement of eq 8, $(V_{V2}^{iso})^{-1/2}$ versus s^2 gives a straight line (Debye plot) in which the correlation length a is obtained by $a = (\lambda/2\pi)(\text{slope/intercept})^{1/2}$. Therefore, by changing the V_{V2}^{iso} value between $(4/3)H_V$ and the observed V_V little by little, V_{V2}^{iso} where the Debye plot became closest to a straight line was determined by a least-squares technique. Figure 5 shows one of the typical Debye plots of the PMMA glasses polymerized at a temperature below the T_g. The experimental data of V_{V2}^{iso} coincide quite well with the Debye plots, which verified the validity using eq 7 for the correlation function $\gamma(r)$ in the PMMA glasses.

The light scattering data of the samples in Figure 4, according to the above analytical procedure, are listed in Table I along with the physical properties. During the polymerization time from 96 to 240 h, α_2^{iso} increased from 41 to 638 dB/km, which was caused by the increase in $\langle\eta^2\rangle$ (from 1.05 × 10^{-8} to 1.13 × 10^{-7}) of the large-size heterogeneities with correlation lengths $a \simeq$ 560–870 Å.

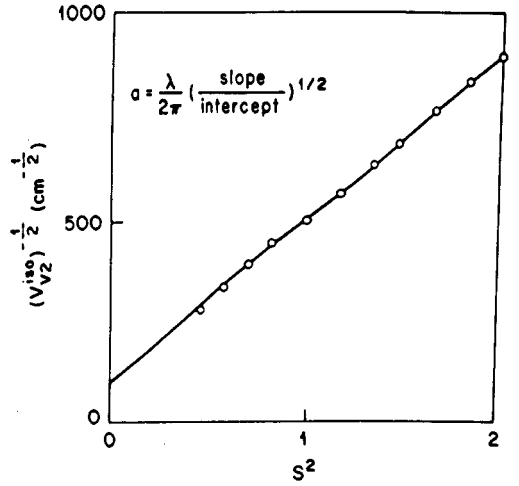

Figure 5. Typical Debye plot of PMMA glass.

These large-size heterogeneities were completely removed by the sufficient heat treatment, and the isotropic scattering loss α_1^{iso} became only 8.9 dB/km (Table I). Here the isotropic scattering loss α^{iso} by the thermal fluctuation theory eq 1 is obtained by the integration of eq 16:

$$\alpha^{iso} = \left(\frac{80 \log e}{27}\right)\frac{\pi^3}{\lambda_0^4}(n^2-1)^2(n^2+2)^2 kT\beta \qquad (19)$$

The calculated α^{iso} value of the PMMA bulk, using the published value[24] of β of 3.55×10^{-11} cm^2/dyn around T_g, is 9.5 dB/km at room temperature for 633-nm wavelength. It should be noted that the α_1^{iso} value of 8.9 dB/km after the heat treatment of sample C is quite close to the theoretical limit 9.5 dB/km. (The fact that the value of 8.9 dB/km is smaller than 9.5 dB/km is probably due to the overestimation[8] of the H_V intensity because of $V_{V1}^{iso} = V_{V1} - (4/3)H_V$ (eq 2).)

In Table I T_g gradually increased from 80 to 102 °C during the polymerization and heat treatment because the remaining monomer decreased from 5.5 to 1.7 wt %. Although the remaining monomer (4.7 wt %) at t_p = 216 h decreased to 1.7 wt % by the heat treatment at 180 °C, the dramatic decrease in α_2^{iso} from 317 to 0 dB/km is not caused by the decrease in the remaining monomer, which was pointed out in our previous paper,[8] but by the relaxation of the heterogeneities above T_g as shown in Figure 4. We believe that the slight amount of decrease in the remaining monomer from 5.5 to 4.0 wt % during the polymerization for t_p = 96–240 h below T_g is the main factor causing the excess scattering, as we shall discuss below.

In Figure 6 the effect of the decrease in the remaining monomer on the excess V_V scattering at $\theta = 60°$ (V_{V60}) is shown, compared with the case of PMMA including a model compound, methyl isobutylate (MIB).

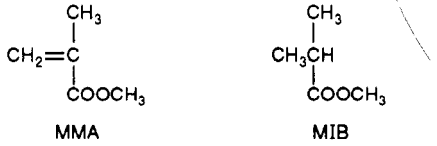

The structure of MIB is quite similar to that of MMA as shown. However, since MIB has no double bond, MIB is not polymerizable and remains unreacted even after complete polymerization. Sample D ($M_w = 8.5 \times 10^4$, T_g = 80 °C) was prepared by polymerizing pure MMA at 70 °C for 96 h; on the other hand, sample E ($M_w = 8.0 \times 10^4$, T_g = 90 °C) was prepared by adding 4 wt % MIB and polymerizing at 130 °C for 96 h. These two samples were heat-treated at 70 °C as shown in Figure 5.

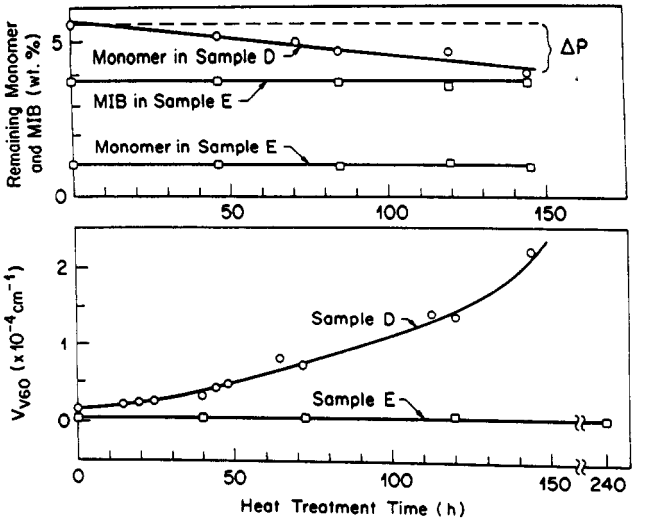

Figure 6. Remaining monomer and MIB concentrations and V_{V60} scattering during heat treatment at 70 °C.

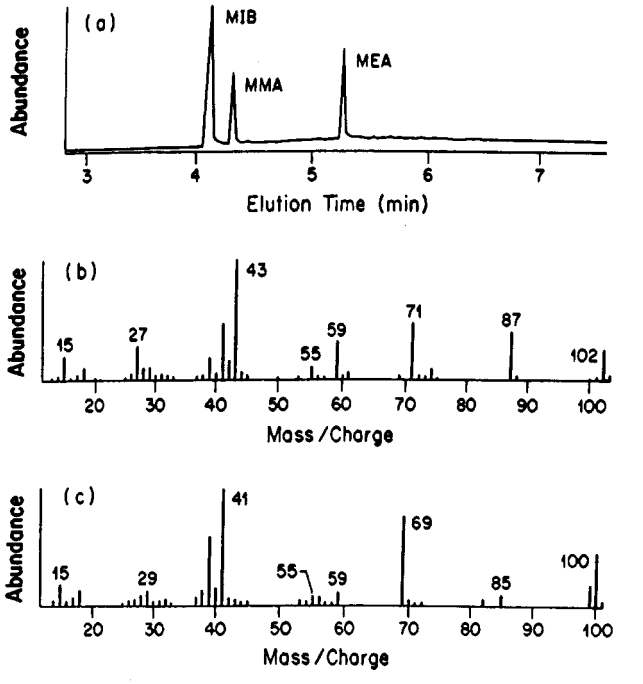

Figure 7. Results of GC/MS for sample E after heat treatment at 70 °C for 144 h: (a) chart of gas chromatography; (b) mass spectrum of MIB at 4.1 min of elution time in (a); (c) mass spectrum of MMA at 4.3 min.

The amounts of the remaining monomer and the monomer model compound (MIB) during the heat treatment in Figure 6 were measured with a gas chromatograph/mass spectrometer (GC/MS). For instance, the results obtained from sample E after the heat treatment are shown in Figure 7 where (a) shows the chart of the gas chromatography, and (b) and (c) show the mass spectra of two peaks at 4.1 and 4.3 min of elution time in (a), respectively.

The mass spectra of (b) and (c) had the parent peaks with 102 and 100 corresponding to the molecular weight of MIB and MMA and were exactly identified, from all fragment peaks, to be MIB and MMA, respectively. Here the peak at 5.3 min is of 2-methoxyethyl acetate (MEA) added in the supernatant of the samples as an internal standard.

It is noteworthy in Figure 6 that the V_{V60} scattering of sample E remain almost constant around 5×10^{-6} cm^{-1}

Table II
Scattering Data and Physical Properties of PMMA Glasses for Case 2

condition	a (Å)	$\langle\eta^2\rangle$ (10^{-8})	V_{V1}^{iso} (10^{-6} cm^{-1})	H_V (10^{-7} cm^{-1})	α_1^{iso} (dB/km)	α_2^{iso} (dB/km)	α^{aniso} (dB/km)	α (dB/km)	density (g/cm^3)	monomer (wt %)
after polymn		0	2.6	3.4	9.5	0	4.1	13.6	1.1880	3.6
heat treatment at 70 °C		0	6.2	4.0	22.5	0	4.8	27.4	1.1909	3.6

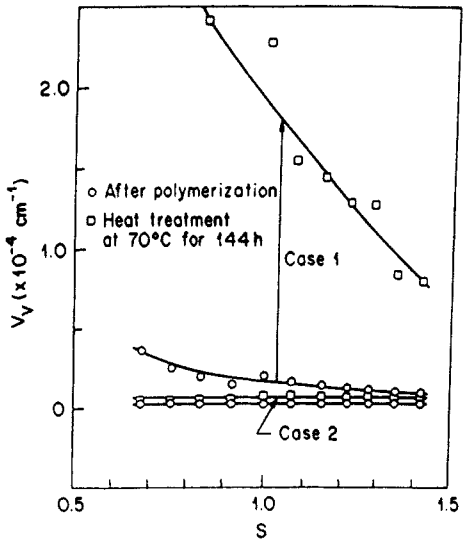

Figure 8. Comparison of V_V scattering before and after heat treatment at 70 °C for 144 h: case 1, polymerized at 70 °C for 96 h; case 2, polymerized at 130 °C for 96 h, 150 °C for 24 h, and 180 °C for 24 h.

during the whole heat treatment period, while the V_{V60} of sample D remarkably increased to 2.2×10^{-4} cm^{-1} after 144 h at 70 °C. Here it should be emphasized that the remaining monomer in sample D decreased almost linearly from 5.5 to 4.0 wt %; on the other hand, the remaining monomer and MIB in sample E remained the same, 1 and 4 wt %, respectively. The refractive indices of MIB, MMA, and PMMA are 1.384, 1.416, and 1.492, and the solubility parameters[25] δ calculated from eq 20 are 7.5, 8.1, and 9.5 (cal/cm^3)$^{1/2}$, respectively.

$$\delta = \frac{\rho \sum G}{M} \tag{20}$$

where ρ is the density, M the molecular weight, and G the molar-attraction constant. Considering the differences of the refractive index and solubility parameter from those of PMMA, the effect of MIB on the excess scattering should be enlarged compared with the real MMA monomer, if aggregation had occurred during heat treatment. Therefore, it was confirmed from the result of sample E in Figure 6 that the remaining monomer in concentrations of up to several weight percent will not spontaneously aggregate to increase the excess V_V scattering during heat treatment below T_g at 70 °C.

In order to rigorously confirm the effect of such a slight amount of polymerization on the excess scattering at high conversion, the following experiment was carried out (see Figure 8). In case 1, the sample that had been polymerized at 70 °C for 96 h (sample D) including 5.5 wt % of the remaining monomer was heat-treated at 70 °C for 144 h. Namely, the two samples before and after the heat treatment in case 1 are the same as the samples at t_p = 96 and 240 h in Table I, respectively. After the heat treatment at 70 °C for 144 h, the remaining monomer decreased to 4.0 wt % and the V_V scattering largely increased, showing besides a stronger angular dependence. On the other hand, the sample in case 2 was polymerized at 130 °C for 96 h, 150 °C for 24 h, and 180 °C for 24 h. The monomer concentration at the end of this treatment was 3.6 wt %. (The remaining monomer after polymerization at 130 °C for 96 h was only 1 wt %; however, after 24 h at 180 °C depolymerization caused the amount of monomer to increase to 3.6 wt %.) The monomer generated by the depolymerization was identified by mass spectrometry as pure MMA. The scattering data and the percent of remaining monomer before and after the heat treatment at 70 °C in case 2 are listed in Table II. As opposed to case 1, little increase in the V_V scattering was observed after the heat treatment at 70 °C, and the remaining monomer before and after the heat treatment remained unchanged (3.6 wt %). Since the remaining initiator (DBPO) had already been consumed after the high-temperature exposure (130 °C for 96 h, 150 °C for 24 h, and 180 °C for 24 h), no polymerization could occur during the heat treatment at 70 °C.

It is concluded that, if the remaining monomer in concentration of several weight percent is not polymerized during the heat treatment below T_g, the aggregation of the monomer giving the excess scattering does not spontaneously occur. We believe that the large increase in the V_V scattering during the heat treatment below T_g is due to the large-size heterogeneities caused by a slight amount of polymerization of the remaining monomer at high conversion. On the basis of these experimental results, we propose an excess scattering model at high conversion.

Excess Scattering Model. The following assumptions are made:

(1) The large-size heterogeneities causing the excess scattering are isotropic structures.

(2) The heterogeneous structure consists of two phases (phases A and B) due to the localization of the monomer, initiator, and void caused by shrinkage during polymerization.

(3) The correlation function is approximated by $\gamma(r) = \exp(-r/a)$ (eq 7).

(4) The Lorentz–Lorenz equation is additive in the polymer–monomer system at high conversion.

Regarding assumption 1, we already mentioned that the H_V intensity was always constant around 5×10^{-7} cm^{-1} and had no angular dependence for any of the PMMA samples prepared in this paper (Figures 2 and 4), which means that no nodular structures such as folded chains exist. Thus, assumption 1 seems reasonable. Concerning assumption 2, the two-phase model[28] assumes a sharp boundary between the two phases. If the structure has a gradient interface[29-31] between the two phases, the scattering intensity deviates from the two-phase model that assumes a sharp boundary. In Porod's region[32] (in the tail of the scattering curve) the effect of the gradient interface on the V_V intensity is not negligible; however, at lower scattering angles than in Porod's region, the scattering curve is insensitive to the interface thickness. In Porod's region, namely, when $(\nu sa) \gg 1$ in eq 8, V_{V2}^{iso} may be written as

$$V_{V2}^{iso} = \frac{\langle\eta^2\rangle}{2\pi n^4} \frac{1}{as^4} \tag{21}$$

where V_{V2}^{iso} is inversely proportional to the correlation

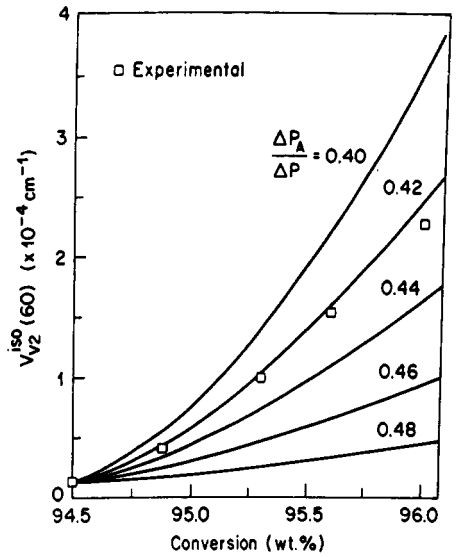

Figure 9. $V_{V2}^{iso}(60)$ as a function of conversion P when a = 700 Å.

length a. On the other hand, at small scattering angles V_{V2}^{iso} increases with a as written in eq 8 and passes through a maximum defined as $\partial V_{V2}^{iso}/\partial a = 0$ which occurs when $s_c = 3^{1/2}\lambda/(2\pi a)$. Here s_c is s when $\partial V_{V2}^{iso}/\partial a = 0$. In our samples, a = 560–870 Å; then s_c = 3.1–2.0 which is larger than the measurement region of $s < 1.4$ used in the data analysis (see Figures 4 and 8) in this paper. Therefore, assumption 2 may be acceptable in our analysis.

As for assumption 3, Figure 5 may show the validity of using the approximation of $\gamma(r) = \exp(-r/a)$ (eq 7) in our study. If the two-phase model with a sharp boundary is assumed, this model leads to $\gamma(r) = \exp(-r/a)$ without any approximation, in which the correlation length a is given by[28]

$$a = (4V/S)v_A v_B \tag{22}$$

where S is the total surface area of the sharp boundary, V is the total volume, and v_A and v_B are the volume fractions of phases A and B, respectively. Therefore, there is no discrepancy between assumptions 2 and 3. In other words, if assumption 2 is used, the approximation of $\gamma(r) = \exp(-r/a)$ should be made.

In case 2 in Table II, the density increased from 1.1880 to 1.1909 by the heat treatment at 70 °C for 144 h. This increase may be caused by the densification due to the aging effect[33] below T_g, which was recognized by a large enthalpy relaxation peak just after the T_g in a DSC chart when increasing the temperature. However, this heat treatment did not increase the light scattering as shown in Table II, which means that the densification during aging does not generate the large-size heterogeneities and is homogeneously caused, details of which will be reported. Therefore, a slight decrease in the free volume by the aging effect is not considered in this model.

In the two-phase model, the mean-square average of the fluctuation of the dielectric constant $\langle\eta^2\rangle$ is given by

$$\langle\eta^2\rangle = (n_A^2 - n^2)^2 v_A + (n_B^2 - n^2)v_B \tag{23}$$

where n_A and n_B are the refractive indices of phases A and B, and n is the average refractive index of the system. If we use assumption 4

$$\frac{n^2-1}{n^2+2} = \frac{n_A^2-1}{n_A^2+2}v_A + \frac{n_B^2-1}{n_B^2+2}v_B \tag{24}$$

On the other hand, if the additivity of the dielectric constants in phases A and B is assumed

$$n^2 = n_A^2 v_A + n_B^2 v_B \tag{25}$$

which corresponds to the Newton equation. In this case $\langle\eta^2\rangle$ in the two-phase model becomes

$$\langle\eta^2\rangle = v_A v_B (n_A^2 - n_B^2)^2 \tag{26}$$

In X-ray and neutron scattering, the equation corresponding to eq 26 has been widely used,[32] except that n_A^2 and n_B^2 are replaced by the corresponding electron densities. However, in order to take into account the polarization effect inherent in the light, we used the Lorentz–Lorenz equation (eq 24), although the difference between the two is small.

Let us first discuss phase A which consists of polymer, monomer, and void. The volume fraction $(\phi_m)_A$ of the monomer in phase A at conversion P is given by

$$(\phi_m)_A = \frac{\zeta_A - \zeta_p(1-(\phi_s)_A)}{\zeta_m - \zeta_p} \tag{27}$$

$$\zeta_A \equiv \frac{n_A^2-1}{n_A^2+2}, \quad \zeta_p \equiv \frac{n_p^2-1}{n_p^2+2}, \quad \zeta_m \equiv \frac{n_m^2-1}{n_m^2+2}$$

where n_m and n_p denote the refractive indices of the monomer and of the polymer, respectively, and $(\phi_s)_A$ is the volume fraction of the void at conversion P due to the density difference between the polymer (1.19) and monomer (0.94) in phase A. The replacement of subscript A with B gives the volume fraction of the monomer in phase B. It is considered that slight amounts of monomer ΔP_A and ΔP_B trapped in phases A and B, respectively, are polymerized in situ without changing the volume of the system, thus generating the voids in the respective phases, and the total conversion P increases to $(P + \Delta P)$, where $\Delta P = \Delta P_A + \Delta P_B$. Then the refractive index $n_A(P + \Delta P)$ in phase A at conversion $(P + \Delta P)$ becomes

$$n_A(P+\Delta P) = \left(\frac{1+2\zeta_A(P+\Delta P)}{1-\zeta_A(P+\Delta P)}\right)^{1/2} \tag{28}$$

$$\zeta_A(P+\Delta P) = \zeta_A + \frac{\Delta P_A}{\left[\frac{P}{\rho_p} + \frac{(1-P)}{\rho_m} + V_s\right]v_A}\left(\frac{\zeta_p}{\rho_p} - \frac{\zeta_m}{\rho_m}\right)$$

where ρ_m and ρ_p are the densities of the monomer and polymer, and V_s is the total volume of the void due to shrinkage in a one-g system at conversion P. By replacing subscript A with B, the refractive index n_B in phase B at conversion $(P + \Delta P)$ is estimated in the same manner. By substituting eq 23 into eq 8, V_{V2}^{iso} becomes

$$V_{V2}^{iso} = \frac{8\pi^2 a^3}{\lambda_0^4(1+\nu^2 s^2 a^2)^2}\{(n_A^2 - n^2)^2 v_A + (n_B^2 - n^2)^2 v_B\} \tag{29}$$

Therefore, by using eqs 24 and 27–29, V_{V2}^{iso} is calculated as a function of conversion P.

Figure 9 shows V_{V2}^{iso} at $\theta = 60°$ against conversion, obtained by calculating the difference between $V_{V2}^{iso}(60)$ at a give conversion and the experimental V_{V2}^{iso} of sample D at P = 94.5 wt % in Figure 6. Here a = 700 Å, $V_s = 0$ at P = 94.5 wt %, and v_A = 0.5. Since there appears to be no trend in the correlation lengths (a) in Table I, we assume a constant value of 700 Å for a. Since $V_{V2}^{iso}(60)$ calculated as the difference with respect to the experimental V_{V2}^{iso} at

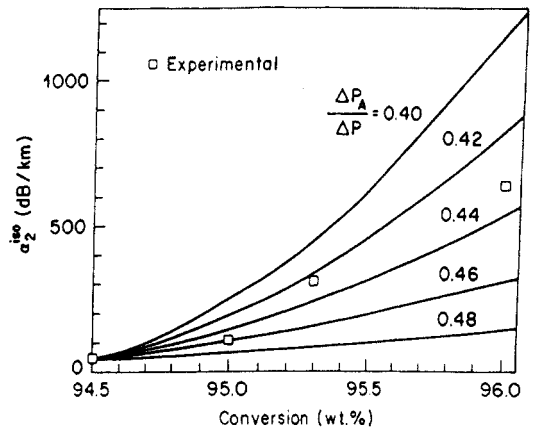

Figure 10. α_2^{iso} as a function of conversion P when a = 700 Å.

P = 94.5 wt % is quite insensitive to V_s, then we assumed V_s = 0 at P = 94.5 wt %. As for v_A, we do not know at present how to determine it from the scattering data. (The effect of v_A on the scattering loss is shown in Figure 11.) It should be noted in Figure 9 that the slope of the V_{V2}^{iso} curve increases with increasing conversion in both the experimental and the calculated data. If $\Delta P_A/\Delta P$ is assumed to be 0.42, void fractions of 0.32 vol % in phase A and of 0.45 vol % in phase B would be generated during the polymerization from 94.5 to 96 wt %, with a concurrent increase in the difference of the refractive indices between phases A and B from 8×10^{-5} to 3×10^{-4}, causing an increase in $V_{V2}^{iso}(60)$ as shown in Figure 9. The dependence of α_2^{iso} on the conversion P was obtained by substituting eq 23 into eq 18 and by using the same procedure for $V_{V2}^{iso}(60)$. The calculated result is shown in Figure 10. It is very interesting that, for instance, when $\Delta P_A/\Delta P$ = 0.42–0.44, a rise of only 1 wt % in the conversion dramatically increases the scattering loss by ca. 500 dB/km.

A general kinetic expression for the rate of radical polymerization is given by

$$-\frac{d[M]}{dt} = (\text{constant})[M][I]^{1/2} \tag{30}$$

where [M] and [I] denote the instantaneous concentrations of monomer and unreacted initiator. When these two concentrations are defined in phases A and B by adding subscripts A and B, respectively, then $\Delta P_A/\Delta P_B$ may be expressed as

$$\frac{\Delta P_A}{\Delta P_B} \simeq \frac{d[M]_A}{d[M]_B} = \frac{[M]_A[I]_A^{1/2}}{[M]_B[I]_B^{1/2}} \tag{31}$$

Therefore, if we know the concentrations of the monomer and initiator in phases A and B, then $\Delta P_A/\Delta P$ in Figures 9 and 10 is obtained. In order to discuss these concentrations, it is important to consider the Flory–Huggins interaction parameter[33,34] χ between the monomer and polymer (χ_{MP}) and between the initiator and polymer (χ_{IP}). The interaction parameter χ is defined by

$$\chi = \frac{(\delta_i - \delta_p)^2}{N_i kT} \tag{32}$$

where subscript i denotes the monomer (i = M) or initiator (i = I) and P the polymer, δ_i and δ_p are the solubility parameters, and N_i is the number of segments per unit volume. When δ_M, δ_I, and δ_P are calculated using eq 20,

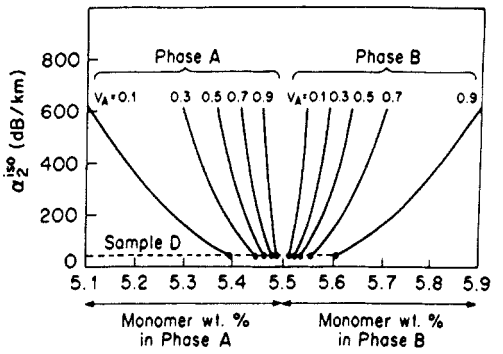

Figure 11. Effect of monomer diffusion between phases A and B on α_2^{iso}.

then the ratio (χ_{MP}/χ_{IP}) becomes

$$\frac{\chi_{MP}}{\chi_{IP}} = \frac{(\delta_M - \delta_P)^2}{(\delta_I - \delta_P)^2} = 0.17 \tag{33}$$

This value implies that the initiator has a much stronger tendency to aggregate than the monomer. (The effect of monomer aggregation on the scattering loss is discussed in Figure 11.) Therefore, it is important to know the amount of initiator which remains unreacted at high conversion.

In general, the radical polymerization is initiated by radicals generated by the decomposition of the initiator. This reaction rate is given by $-d[I]/dt = k[I]$. Since the reaction constant k can be described by the Arrhenius equation, the kinetics of initiator decomposition is given by

$$\ln([I]/[I]_0) = -A \exp(-\Delta E/RT)t \tag{34}$$

where ΔE is the activation energy of the decomposition of the initiator into primary radicals, A the frequency factor, $[I]_0$ the concentration of the initiator at t = 0, and R the gas constant. Here ΔE = 37.3 kcal/mol and $A = 2.41 \times 10^{19}$ h for DBPO.[35] Then, the concentrations of the unreacted initiator in case 1 (polymerized at 70 °C for 96 h) and case 2 (polymerized at 130 °C for 96 h, 150 °C for 24 h, and 180 °C for 24 h) before the heat treatment are

$$[I]/[I]_0 = 0.996 \quad \text{in case 1}$$

$$[I]/[I]_0 = 0.000 \quad \text{in case 2} \tag{35}$$

It is noteworthy that almost all the initiator in case 1 (sample D) remains unreacted, but in case 2 its concentration is 0%, which strongly corroborates the conclusion mentioned above in Figure 8 and Table II. Although we cannot obtain the absolute concentrations of the monomer and initiator in eq 31, it should be concluded from eqs 33 and 35 that the remaining monomer trapped in the solidified polymer glasses at high conversion may be heterogeneously polymerized due to the aggregated initiator which remains unreacted, increasing the scattering loss as shown in Figure 10.

So far we have discussed the effect of the void concentration generated at high conversion assuming that the monomer trapped in phases A and B is polymerized in situ without any monomer diffusion. However, as an additional effect, we should also consider the effect of the monomer diffusion. Figure 11 shows the effect of the monomer migration between phases A and B on α_2^{iso} without considering the void effect. Since we cannot determine v_A, several cases with different v_A values are shown. Closed circles show the monomer concentrations

in phases A and B for sample D polymerized at 70 °C for 96 h. For instance, in the case of $v_A = 0.5$, when the monomer concentration in phase A decreases from 5.46 wt % (sample D) to 5.40 wt % by migration, α_2^{iso} increases from 43 to 340 dB/km. However, it is again emphasized that such a migration may not occur spontaneously unless a slight amount of monomer at high conversion is polymerized, which is clearly the case as pointed out by Figures 6 and 8 and eq 35. We believe that, if monomer migration is additionally caused, the driving force might be the volume shrinkage that accompanies polymerization, which would cause monomer to be squeezed out of the shrinking domain.

Conclusions

The origin of the excess light scattering observed in purified PMMA glasses was investigated.

(1) The large-size heterogeneities causing the excess scattering of several hundred dB/km are the isotropic structures with a correlation length of several hundred angstroms and are not due to extrinsic impurities, high molecular weight, formation of cross-links, specific tacticities, or aging.

(2) The heterogeneous structure is generated during the polymerization below T_g at high conversion but disappears after a long enough heat treatment above T_g.

(3) The large increase in the V_V scattering at high conversion is due to a slight amount of polymerization of the remaining monomer trapped inside the polymer glass.

(4) Aggregation of the remaining monomers giving the excess scattering does not occur spontaneously during the heat treatment below T_g, unless a slight amount of polymerization takes place.

(5) The excess scattering model proposed in this paper shows that if a slight amount of monomer trapped inside the PMMA glass is polymerized in situ, generating slightly localized voids due to the aggregation of the unreacted initiator (eqs 31, 33, and 35), a 1 wt % rise in the conversion around $P = 95$ wt % increases the scattering loss by several hundred dB/km, which quite reasonably explains all experimental results obtained in this paper.

Acknowledgment. We gratefully acknowledge G. E. Johnson, F. Houlihan, X. Quan, A. Hale, Dr. Ohtsuka, and Dr. Tanio for many valuable discussions.

References and Notes

(1) Fischer, E. W.; Dettenmaier, M. *J. Non-Cryst. Solids* **1978**, *31*, 181.
(2) Misra, A.; David, D. J.; Snelgrove, J. A.; Matis, G. *J. Appl. Polym. Sci.* **1986**, *31*, 2387.
(3) Yamashita, T.; Shichijyo, S.; Takemura, T.; Matsushige, K. *Jpn. J. Appl. Phys., Part 2* **1987**, *26*, L1797.
(4) Cielo, D.; Favis, B. D.; Maldague, X. *Polym. Eng. Sci.* **1987**, *27*, 1601.
(5) Judd, R. E.; Crist, B. *J. Polym. Sci., Polym. Lett. Ed.* **1980**, *18*, 717.
(6) Koberstein, J.; Stein, R. S. *Polymer* **1984**, *25*, 171.
(7) Fujiki, M.; Kaino, T.; Oikawa, S. *Polym. J.* **1983**, *15*, 693.
(8) Koike, Y.; Tanio, N.; Ohtsuka, Y. *Macromolecules* **1989**, *22*, 1367.
(9) Imoto, K.; Sano, H.; Maeda, M. *Appl. Opt.* **1986**, *25*, 3443.
(10) Goodwin, M. J. *SPIE* **1987**, *836*, 265.
(11) Koike, Y.; Takezawa, Y.; Ohtsuka, Y. *Appl. Opt.* **1988**, *27*, 486.
(12) Emslie, C. *J. Mater. Sci.* **1988**, *23*, 2281.
(13) Kaino, T. *J. Polym. Sci., Part A* **1987**, *25*, 37.
(14) Koike, Y. *Polymer* **1991**, *32*, 1737.
(15) Fischer, E. W.; Wendorff, J. H.; Dettenmaier, M.; Lieser, G.; Voigt-Martin, I. *J. Macromol. Sci., Phys.* **1976**, *B12*, 41.
(16) Dettenmaier, M.; Fischer, E. W. *Kolloid-Z. Z. Polym.* **1973**, *251*, 922.
(17) Shichijyo, S.; Matsushige, K.; Takemura, T. *Mem. Fac. Eng., Kyushu Univ.* **1985**, *45*, 225.
(18) Einstein, A. *Ann. Phys.* **1910**, *33*, 1275.
(19) Tanio, N.; Koike, Y.; Ohtsuka, Y. *Polym. J.* **1989**, *21*, 259.
(20) Meeten, G. H. *Optical Properties of Polymers*; Elsevier Applied Science Publishers: London, 1986.
(21) Debye, P.; Bueche, A. M. *J. Appl. Phys.* **1949**, *20*, 518.
(22) Kerker, M. *The Scattering of Light and Other Electromagnetic Radiation*; Academic Press: New York, 1972.
(23) Tanio, N.; Koike, Y.; Ohtsuka, Y. *Polym. J.* **1989**, *21*, 119.
(24) Matsuoka, S.; Bair, H. E. *J. Appl. Phys.* **1977**, *48*, 4058.
(25) *Polymer Handbook*; Brandrup, J., Immergut, E. H., Eds.; Wiley-Interscience: New York, 1975; p II-421.
(26) Reference 25, p V-55.
(27) Reference 25, p IV-339.
(28) Debye, P.; Anderson, H. R.; Brumberger, H. *J. Appl. Phys.* **1957**, *28*, 679.
(29) Hashimoto, T.; Todo, A.; Itoi, H.; Kawai, H. *Macromolecules* **1977**, *10*, 377.
(30) Roe, R. J.; Fishkis, M.; Chang, J. C. *Macromolecules* **1981**, *14*, 1091.
(31) Koberstein, J. T.; Stein, R. S. *J. Polym. Sci., Polym. Phys. Ed.* **1983**, *21*, 1439.
(32) Glatter, O.; Kratky, O. *Small Angle X-ray Scattering*; Academic Press: London, 1982.
(33) Matsuoka, S.; Williams, G.; Johnson, G. E.; Anderson, E. W.; Furukawa, T. *Macromolecules* **1985**, *18*, 2652.
(34) Ronca, G.; Russell, T. P. *Phys. Rev. B* **1987**, *35*, 8566.
(35) Olvera de la Cruz, M.; Edwards, S. F.; Sanchez, I. C. *J. Chem. Phys.* **1988**, *89*, 1704.
(36) Catalog of Organic Peroxides in Nippon Oil & Fats Co., Ltd.

Registry No. PMMA, 9011-14-7.